

SUPPLEMENTAL INFORMATION

Automatic local resolution-based sharpening of cryo-EM maps

Erney Ramírez-Aportela^{a,†,*}, Jose Luis Vilas^{a,†}, Alisa Glukhova^b, Roberto Melero^a, Pablo Conesa^a, Marta Martínez^a, David Maluenda^a, Javier Mota^a, Amaya Jiménez^a, Javier Vargas^c, Roberto Marabini^d, Patrick M. Sexton^{b,e}, Jose Maria Carazo^{a,*}, Carlos Oscar S. Sorzano^{a,f,*}

^aBiocomputing Unit, National Center for Biotechnology (CSIC), Darwin 3, Campus Univ. Autónoma de Madrid, 28049 Cantoblanco, Madrid, Spain.

^bDrug Discovery Biology, Monash Institute of Pharmaceutical Sciences, Parkville 3052, Victoria, Australia.

^cDept of Anatomy and Cell Biology, McGill University, 3640 Rue University, Montreal, Canada.

^dUniv. Autónoma de Madrid, Campus Univ. Autónoma de Madrid, 28049 Cantoblanco, Madrid, Spain.

^eSchool of Pharmacy, Fudan University, Shanghai 201203, China.

^fUniv. CEU San Pablo, Campus Urb. Montepríncipe, Boadilla del Monte, 28668 Madrid, Spain.

[†]These two authors have equally contributed to this work.

*Correspondence should be addressed to E.R-A. (erney.ramirez@gmail.com), J.M.C. (carazo@cnb.csic.es) and C.O.S.S. (cooss@cnb.csic.es).

The matrix product HX is equal to the convolution results:

$$\begin{pmatrix}
 h_{0,0}x_1 + h_{0,1}x_2 + h_{1,0}x_6 + h_{1,1}x_7 \\
 h_{0,-1}x_1 + h_{0,0}x_2 + h_{0,1}x_3 + h_{1,-1}x_6 + h_{1,0}x_7 + h_{1,1}x_8 \\
 h_{0,-1}x_2 + h_{0,0}x_3 + h_{0,1}x_4 + h_{1,-1}x_7 + h_{1,0}x_8 + h_{1,1}x_9 \\
 h_{0,-1}x_3 + h_{0,0}x_4 + h_{0,1}x_5 + h_{1,-1}x_8 + h_{1,0}x_9 + h_{1,1}x_{10} \\
 h_{0,-1}x_4 + h_{0,0}x_5 + h_{1,-1}x_9 + h_{1,0}x_{10} \\
 h_{-1,0}x_1 + h_{-1,1}x_2 + h_{0,0}x_6 + h_{0,1}x_7 + h_{1,0}x_{11} + h_{1,1}x_{12} \\
 h_{-1,-1}x_1 + h_{-1,0}x_2 + h_{-1,1}x_3 + h_{0,-1}x_6 + h_{0,0}x_7 + h_{0,1}x_8 + h_{1,-1}x_{11} + h_{1,0}x_{12} + h_{1,1}x_{13} \\
 h_{-1,-1}x_2 + h_{-1,0}x_3 + h_{-1,1}x_4 + h_{0,-1}x_7 + h_{0,0}x_8 + h_{0,1}x_9 + h_{1,-1}x_{12} + h_{1,0}x_{13} + h_{1,1}x_{14} \\
 h_{-1,-1}x_3 + h_{-1,0}x_4 + h_{-1,1}x_5 + h_{0,-1}x_8 + h_{0,0}x_9 + h_{0,1}x_{10} + h_{1,-1}x_{13} + h_{1,0}x_{14} + h_{1,1}x_{15} \\
 h_{-1,-1}x_4 + h_{-1,0}x_5 + h_{0,-1}x_9 + h_{0,0}x_{10} + h_{1,-1}x_{14} + h_{1,0}x_{15} \\
 h_{-1,0}x_6 + h_{-1,1}x_7 + h_{0,0}x_{11} + h_{0,1}x_{12} + h_{1,0}x_{16} + h_{1,1}x_{17} \\
 h_{-1,-1}x_6 + h_{-1,0}x_7 + h_{-1,1}x_8 + h_{0,-1}x_{11} + h_{0,0}x_{12} + h_{0,1}x_{13} + h_{1,-1}x_{16} + h_{1,0}x_{17} + h_{1,1}x_{18} \\
 h_{-1,-1}x_7 + h_{-1,0}x_8 + h_{-1,1}x_9 + h_{0,-1}x_{12} + h_{0,0}x_{13} + h_{0,1}x_{14} + h_{1,-1}x_{17} + h_{1,0}x_{18} + h_{1,1}x_{19} \\
 h_{-1,-1}x_8 + h_{-1,0}x_9 + h_{-1,1}x_{10} + h_{0,-1}x_{13} + h_{0,0}x_{14} + h_{0,1}x_{15} + h_{1,-1}x_{18} + h_{1,0}x_{19} + h_{1,1}x_{20} \\
 h_{-1,-1}x_9 + h_{-1,0}x_{10} + h_{0,-1}x_{14} + h_{0,0}x_{15} + h_{1,-1}x_{19} + h_{1,0}x_{20} \\
 h_{-1,0}x_{11} + h_{-1,1}x_{12} + h_{0,0}x_{16} + h_{0,1}x_{17} + h_{1,0}x_{21} + h_{1,1}x_{22} \\
 h_{-1,-1}x_{11} + h_{-1,0}x_{12} + h_{-1,1}x_{13} + h_{0,-1}x_{16} + h_{0,0}x_{17} + h_{0,1}x_{18} + h_{1,-1}x_{21} + h_{1,0}x_{22} + h_{1,1}x_{23} \\
 h_{-1,-1}x_{12} + h_{-1,0}x_{13} + h_{-1,1}x_{14} + h_{0,-1}x_{17} + h_{0,0}x_{18} + h_{0,1}x_{19} + h_{1,-1}x_{22} + h_{1,0}x_{23} + h_{1,1}x_{24} \\
 h_{-1,-1}x_{13} + h_{-1,0}x_{14} + h_{-1,1}x_{15} + h_{0,-1}x_{18} + h_{0,0}x_{19} + h_{0,1}x_{20} + h_{1,-1}x_{23} + h_{1,0}x_{24} + h_{1,1}x_{25} \\
 h_{-1,-1}x_{14} + h_{-1,0}x_{15} + h_{0,-1}x_{19} + h_{0,0}x_{20} + h_{1,-1}x_{24} + h_{1,0}x_{25} \\
 h_{-1,0}x_{16} + h_{-1,1}x_{17} + h_{0,0}x_{21} + h_{0,1}x_{22} \\
 h_{-1,-1}x_{16} + h_{-1,0}x_{17} + h_{-1,1}x_{18} + h_{0,-1}x_{21} + h_{0,0}x_{22} + h_{0,1}x_{23} \\
 h_{-1,-1}x_{17} + h_{-1,0}x_{18} + h_{-1,1}x_{19} + h_{0,-1}x_{22} + h_{0,0}x_{23} + h_{0,1}x_{24} \\
 h_{-1,-1}x_{18} + h_{-1,0}x_{19} + h_{-1,1}x_{20} + h_{0,-1}x_{23} + h_{0,0}x_{24} + h_{0,1}x_{25} \\
 h_{-1,-1}x_{19} + h_{-1,0}x_{20} + h_{0,-1}x_{24} + h_{0,0}x_{25}
 \end{pmatrix} = \begin{pmatrix} y_1 \\ y_2 \\ y_3 \\ y_4 \\ y_5 \\ y_6 \\ y_7 \\ y_8 \\ y_9 \\ y_{10} \\ y_{11} \\ y_{12} \\ y_{13} \\ y_{14} \\ y_{15} \\ y_{16} \\ y_{17} \\ y_{18} \\ y_{19} \\ y_{20} \\ y_{21} \\ y_{22} \\ y_{23} \\ y_{24} \\ y_{25} \end{pmatrix}$$

The output vector can be reshaped into a 2D form. This is the same result that would be obtained by making a sliding window of h over x .

$$\begin{pmatrix} h_{-1,-1} & h_{-1,0} & h_{-1,1} \\ h_{0,-1} & h_{0,0} & h_{0,1} \\ h_{1,-1} & h_{1,0} & h_{1,1} \end{pmatrix} * \begin{pmatrix} x_1 & x_2 & x_3 & x_4 & x_5 \\ x_6 & x_7 & x_8 & x_9 & x_{10} \\ x_{11} & x_{12} & x_{13} & x_{14} & x_{15} \\ x_{16} & x_{17} & x_{18} & x_{19} & x_{20} \\ x_{21} & x_{22} & x_{23} & x_{24} & x_{25} \end{pmatrix} = \begin{pmatrix} y_1 & y_2 & y_3 & y_4 & y_5 \\ y_6 & y_7 & y_8 & y_9 & y_{10} \\ y_{11} & y_{12} & y_{13} & y_{14} & y_{15} \\ y_{16} & y_{17} & y_{18} & y_{19} & y_{20} \\ y_{21} & y_{22} & y_{23} & y_{24} & y_{25} \end{pmatrix}$$

Transpose filters

Given a filter operation described by a matrix multiplication $Y=HX$, the matrix H is Toeplitz and square (assuming that the output is kept at the same size as the input). This filter can be described in terms of the 2D signals

$$y(\mathbf{r}) = h(\mathbf{r}) * x(\mathbf{r})$$

It can be easily proven that the filter $Y=H^T X$ corresponds to the filtering with a symmetrized version of the filter

$$y(\mathbf{r}) = h(-\mathbf{r}) * x(\mathbf{r})$$

If the filter is even, like a Gaussian filter, for instance, then $h(-\mathbf{r}) = h(\mathbf{r})$ and the transpose filter fulfills $H^T=H$, that is, applying the same filter again.

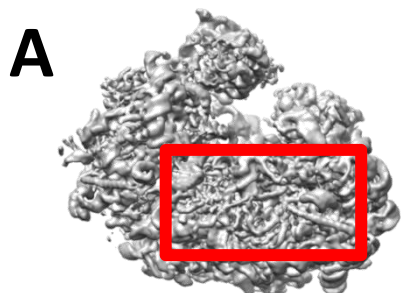
Raised cosine filter

In our approach we apply a filter bank to the map v_{sh} . Each filter in the bank is a bandpass filter centered at frequency ω_i , and represented by a matrix H^i . The filter bank consists of a set of raised cosine filters that cover the frequencies range corresponding to the minimum and maximum resolution determined for the input map, and distributed every 0.2 \AA of resolution. Each raised cosine filter is defined by:

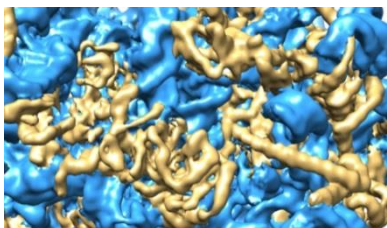
$$h_i(\omega) = \begin{cases} \frac{1}{2} \left(1 + \cos \left(\frac{\pi}{\delta} (\omega_i - \omega) \right) \right) & \omega_i - \delta \leq \omega < \omega_i + \delta \\ 0 & \textit{otherwise} \end{cases}$$

where δ is the width of the transition band (in our experiments we chose $\delta = \omega_\delta - \omega_i$; where $\omega_\delta = 1/(R_i - 0.2)$). Note that the formula above is defined only for positive frequencies ($\omega > 0$). The filter in real space is real-valued and consequently for the negative frequencies it is defined as $h_i(-\omega) = h_i^*(\omega)$. Note also that the definition of the filter is one-dimensional, so that ω represents the norm of the 3D frequency coming from the 3D Fourier transform of the volume.

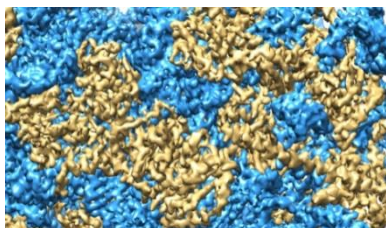
Supplementary Figure 1



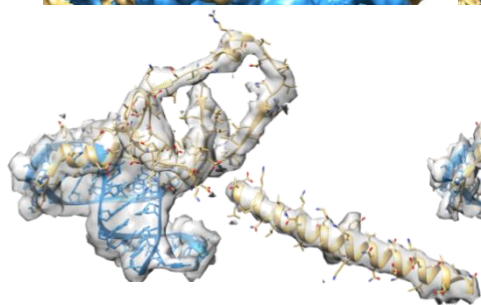
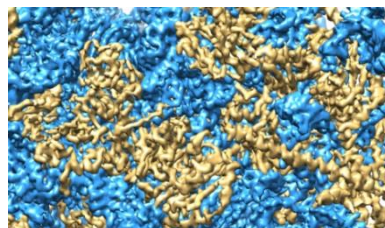
B unsharpened



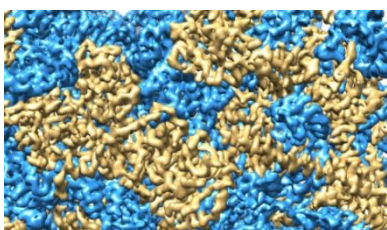
RELION



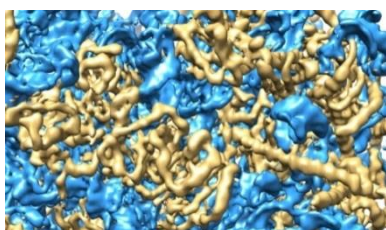
Phenix



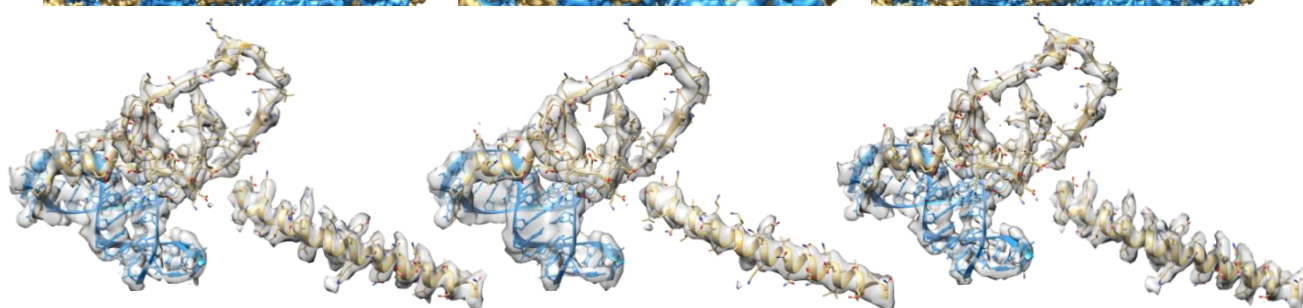
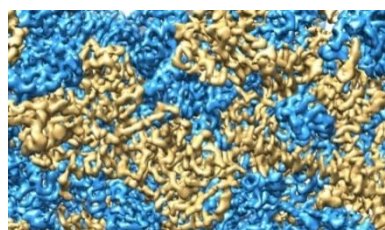
LocalDeblur



LocScale



LocalDeblur+LocScale

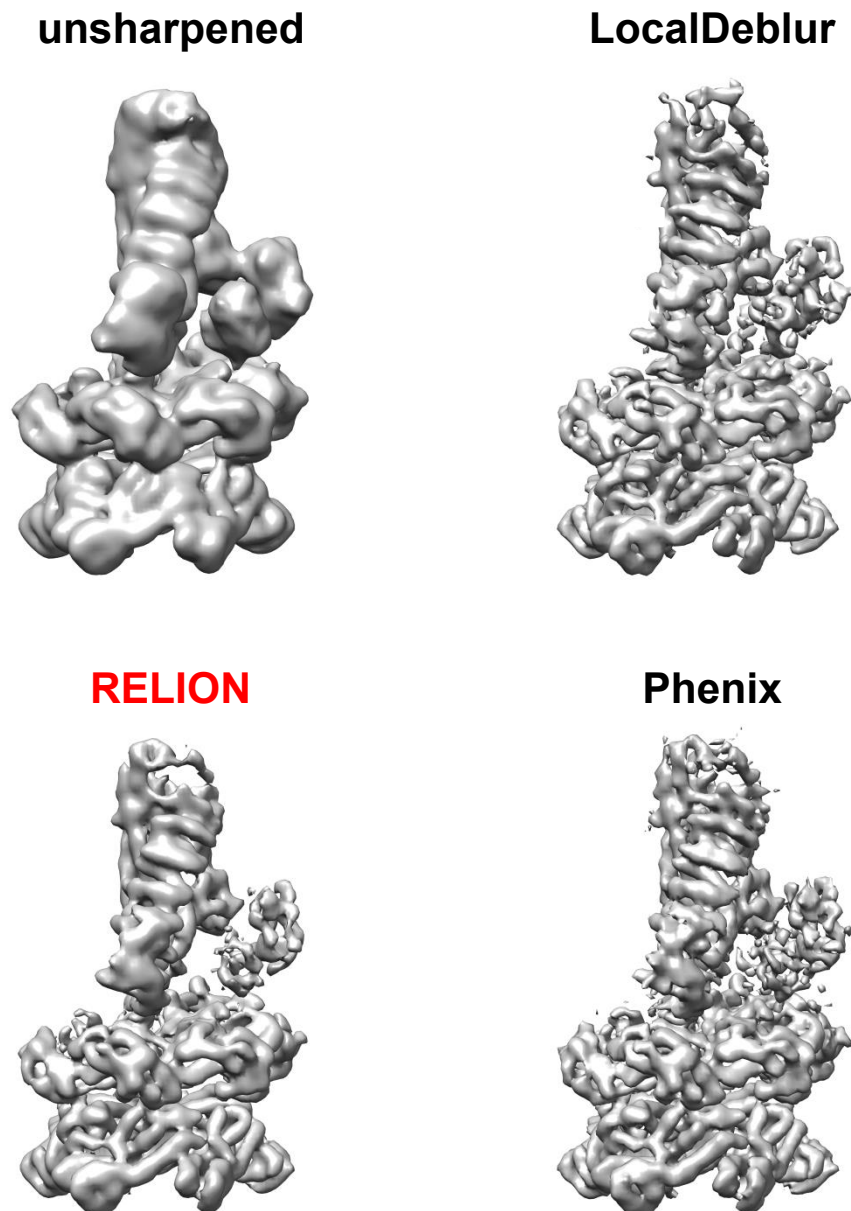


Supplementary Figure 1.

Sharpened maps of *Plasmodium falciparum* 80S ribosome (EMD-2660). (A) The whole density map from 80S ribosome is shown. The red frame corresponds to the density enlarged in panel B.

(B) Sharpened map of 80S ribosome generated with LocalDeblur and comparison with the main sharpening methods (**RELION** post-processing, Phenix AutoSharpen and LocScale). Only the section corresponding to the red frame in A is shown. The RNA density is represented in blue and the amino acid density in yellow. Below each sharpened map, the density for 149-186 (chain-K) (left), and 3712-3727, 3761-3775 (chain-A) and 283-381 (chain-E) (right) residues are represented.

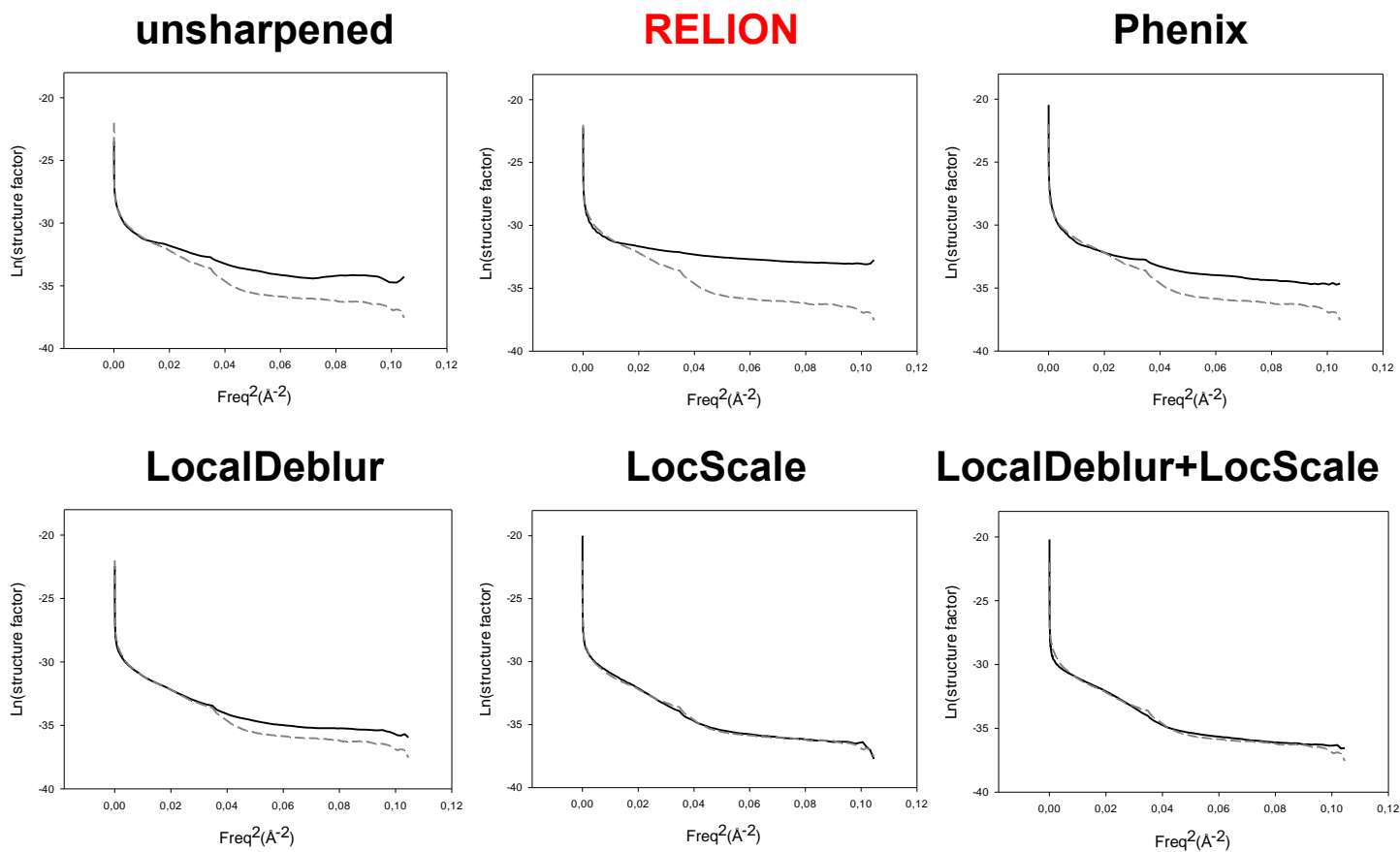
Supplementary Figure 2



Supplementary Figure 2.

Sharpened of low resolution map of L-20S (NSF/ α SNAP/L-SNARE) complex (EMD-8944).

Supplementary Figure 3



Supplementary Figure 3.

Guinier plots for each sharpened map represented in Supplementary Figure 2 are shown. The profile corresponding to the density map generated from the atomic models (PDBs ID: 3j7a and ID: 3j79) is superimposed as a dashed line representing our “target result”. Note how profiles obtained by LocalDeblur are very similar to the target ones.

Supplementary Table 1

TRPV1^a refinement statistics.

	EMDB	LocalDeblur	Phenix	RELION	LocScale	LocalDeblur +LocScale
EMRinger score	2.16	4.12	3.89	3.66	3.40	3.83
Molprobit score	2.19	1.50	1.88	1.72	2.17	2.14
Clashscore	4.71	2.61	3.61	5.37	4.21	3.56
Ramachandran Favored (%) allowed(%)	93.16 6.84	93.13 6.87	92.83 7.17	93.49 6.51	93.81 6.19	93.16 6.84
Rotmers outliers (%)	3.40	0.75	0.75	0.75	1.23	1.13
CC_{mask}	0.80	0.80	0.75	0.73	0.80	0.80

^a ankyrin domain not included